JOURNAL OF GENERAL VIROLOGY

RESEARCH ARTICLE

Büscher *et al.*, *Journal of General Virology* 2025;106:002167
DOI 10.1099/jgv.0.002167

MICROBIOLOGY SOCIETY

OPEN ACCESS

Mutation of the nuclear localization signals of the major tegument protein pp65 leads to impairment of human cytomegalovirus progeny production

Nicole Büscher[1], Christian Sinzger[2], Caroline Lehmann[1], Christine Zimmermann[1], Hanno Schmidt[1,†] and Bodo Plachter[1,*,†]

Abstract

The phosphoprotein 65 (pp65, pUL83) of human cytomegalovirus (HCMV) serves several functions during the viral life cycle. It is one of the most abundant constituents of the virion tegument and the major component of subviral particles termed Dense Bodies. It is also one of several tegument proteins that mediate the subversion of cellular antiviral defence functions like the induction of IFNs. It is also involved in the transcriptional activation of the major immediate early IE1/IE2 gene. Despite its strong nucleophilic nature, pp65 is found in the cytoplasm at late stages of infection. We have previously shown that the nuclear retention phenotype of a mutated pp65 is associated with a distinct deficit in viral productivity. In this study, we generated HCMV mutant viruses in which the nuclear localization signals (nls) of pp65 were mutated, thus preventing nuclear entry and pp65 shuttling. Since the genetic manipulation of UL83 led to the deregulation of the adjacent pp71 gene in initial experiments, we chose to express pp65 with mutated nls from a distant locus within the genome of a TB40/e strain derivative. This virus, termed v65stop-pp65*nls*, was significantly impaired in its capacity to produce infectious progeny. Using knockout fibroblast cells for the DNA sensors IFI16 or cGAS, no differences were seen when progeny production was compared between v65stop-pp65*nls* and a strain expressing wt pp65. Thus, differences in the known subversive effect on these DNA sensors could not account for the differences seen in productivity. Surprisingly, the upload of pp65 into virions and the synthesis of subviral Dense Bodies were abrogated by the mutation of its nls. Although an impairment of pp65 interaction with other proteins by the mutations cannot be excluded, the data suggest that the migration of pp65 through the nucleus was important for HCMV progeny production and packaging.

INTRODUCTION

The human cytomegalovirus (HCMV) is a clinically important pathogen that causes severe disease conditions in pre- or perinatally infected infants and in immunosuppressed individuals [1, 2]. The development of novel antiviral therapeutics is an urgent subject. A central issue of research interest in this respect focusses on our understanding of how viral proteins interact with each other and with cellular factors to ensure viral replication and progeny production. One protein that has been in the focus of such studies is the phosphoprotein 65 (pp65; pUL83). The pp65 is the most abundant tegument protein of mature virions and the major component of subviral particles termed Dense Bodies [3–5]. It is dispensable for HCMV growth in fibroblast culture, but is important for replication in macrophages [6, 7]. The protein is swiftly translocated to the cell nucleus following infection, mediated by three nuclear localization signals (nls) [8, 9]. It interferes with intrinsic defence mechanisms of the cell by impairing DNA sensors, like the cyclic GMP/AMP synthase (cGAS), the IFN-inducible protein 16 (IFI16) and the absent in melanoma 2 protein (AIM2) [10–13]. It also impairs IL-1β expression by modulating gene expression through enhancing NF-κB binding [14], reviewed in [15]. By interacting with IFI16, pp65 stimulates the activity of the viral major immediate-early promoter [16]. Both cytoplasmic and nuclear processes are thus targeted by pp65. Strikingly, pp65 has also been identified as a nucleo-cytoplasmic shuttle protein

Received 20 August 2025; Accepted 10 October 2025; Published 21 October 2025
Author affiliations: [1]Institute for Virology and Research Center for Immunotherapy, University Medical Center of the Johannes Gutenberg-University Mainz, Mainz, Germany; [2]Institute for Virology, Ulm University Medical Center, Ulm, Germany.
***Correspondence:** Bodo Plachter, plachter@uni-mainz.de
Keywords: human cytomegalovirus; nuclear localization; nucleocytoplasmic shuttling; pp65; viral morphogenesis.
Abbreviations: cVAC, cytoplasmic viral assembly compartments; HCMV, human cytomegalovirus; HFF, human foreskin fibroblast; IFI16, IFN-inducible protein 16; ISG, IFN-stimulated gene; NIEPs, non-infectious enveloped particles; nls, nuclear localization signals.
†These authors share senior authorship.

[17, 18]. Consequently, it appears that the presence of the protein in both the nucleus and the cytoplasm in HCMV-infected cells is important for viral replication.

A well-established difference between HCMV low passage strains and the more frequently studied laboratory strains relates to the expression levels and late subcellular localization of pp65. Laboratory strains express high levels of pp65, and most of the pp65 signal, using indirect immunofluorescence assays and specific antibodies, shifts to the cytoplasm in late-stage infected human foreskin fibroblast (HFF). Low-passage HCMV strains, in contrast, express rather moderate levels of pp65 [19]. The TB40/e strain shares characteristics of low-passage HCMV and was thus used here as a model. We have shown before that a viral mutant expressing a modified, preferentially nuclear version of pp65 was severely impaired in progeny release [20]. In this work, we mutated the nls of pp65 to abrogate nuclear entry. We show that these viruses are significantly impaired in their capacity to release progeny even below levels seen with pp65-null mutants. The results suggest that the shuttling function of pp65 is critical for HCMV productivity.

METHODS

Cells, bacterial artificial chromosome cloning and viruses

Primary HFFs and HFF-ko cells were cultured as described before [21, 22]. Retinal pigment epithelial cells (ARPE-19) were obtained from ATCC and were cultured in Dulbecco's Modified Eagle Medium+Ham's F12 medium (1:1), supplemented with 10% v/v fetal calf serum (FCS). Human umbilical vein endothelial cells, conditionally immortalized with tetracycline-dependent expression of the SV40 large-T antigen (HEC-LTT), were cultured as described previously [23, 24]. For growth, HEC-LTTs were cultured in endothelial cell growth medium (EGM BulletKit, Lonza) supplemented with 2 mg ml^{-1} doxycycline (AppliChem, Darmstadt, Germany); for infection experiments, doxycycline was omitted, leading to a permissive state of the cells to HCMV infection [23]. All HCMV strains used in this analysis were derived from bacterial artificial chromosome (BAC) clones.

For the generation of viral mutants, a PCR fragment was generated, using the plasmid pgalK as a template [25]. For the construction of TB40-pp65*nls*, the PCR product was inserted into the BAC TB40-BAC$_{KL7}$ [26], using the GalK selection procedure [25], thereby deleting the UL83 ORF. The resulting BAC construct was then used to generate the BAC clones for TB40E-pp65*nls*. For this, the mutated sequence, including the sequences necessary for recombination, was obtained by custom synthesis from GenScript (Nanjing, Jiangsu, China) and transformed into the bacteria harbouring the galK BAC intermediates. Recombinant clones were selected according to Warming *et al.* [25]. One of the resulting BAC clones was then reconstituted by transfecting BAC DNA into HFF. BACmid DNA for transfection was obtained from *Escherichia coli* using the Plasmid Purification Kit (Macherey-Nagel, Düren, Germany) according to the manufacturer's instructions. Transfections into HFF were performed using the Superfect transfection reagent (Qiagen, Venlo, Netherlands). HFFs, transfected with different amounts of BAC-DNA, were seeded on six-well plates at a density of 1×10^5 cells/well. Cells were subsequently passaged until plaques became visible. The infectious supernatant was then transferred to uninfected cells for the passaging of the virus.

The construction of viruses based on the mutant strain v65stop [7] was performed accordingly. Here, the galK expression cassette was inserted into the UL1-UL6 gene region of that strain [26], thereby deleting the genes in that region. Both the pp65-wt gene sequence and the mutated pp65*nls* sequence were purchased from BioCat (Heidelberg, Germany). The expression of pp65 or pp65*nls* from the reconstituted viruses was verified by indirect immunofluorescence analysis. All HCMV strains were propagated on HFF. Viral stocks were obtained by collecting the culture supernatants from infected HFF, followed by low-speed centrifugation to remove cell debris. Supernatants were frozen at −80 °C until further use.

Levels of viral progeny released in the cell culture supernatant after infection of HFF or ARPE19 were determined by the IE1 titration assay according to Andreoni *et al.* [27]. For this, 5×10^3 HFF cells were seeded in each well of a 96-well plate. The following day, virus-containing culture supernatants were diluted from 10^{-1} to 10^{-4} in culture medium and were added to the cells in octuplet replicates. Cells were fixed after 48 h for 20 min using 96% ethanol. The primary antibody p63-27 [28], kindly provided by William Britt, was added for 1 h in a humidified chamber at 37 °C. Detection was performed by adding an anti-mouse IgG, coupled to horseradish peroxidase (Rabbit-anti-Mouse Immunoglobulin HRP; Dako) at a dilution of 1:500 for 1 h and by subsequent staining with 3-amino-9-ethyl-carbazol/H_2O_2 for another hour. IE1-positive cells were counted and titres were determined as means of octuplet values. For HEC-LTT, the quantitation of virus release was performed as described before [23].

Indirect immunofluorescence analysis, immunoblotting and virion purification

Indirect immunofluorescence and immunoblot analyses were performed as previously published [29, 30]. Virion and Dense Body purification was performed according to Roby and Gibson [3]. Briefly, HFFs were seeded in 175 cm^2 cell culture flasks at a cell density of 1.8×10^6 cells per vessel. Cells were kept in an incubator (5% CO_2; 90% humidity) at 37 °C for 24 h. The cells were then infected with either HCMV strain at a multiplicity of infection of roughly 0.5 /cell. After 6–7 days, depending on visual inspection of the cytopathic effect, the culture supernatants were collected and centrifuged at 1,300 ***g*** for 10 min at room temperature. After that, the supernatants were collected and centrifuged at 100,000 ***g*** (70 min, 10 °C) in an SW32Ti rotor. Meanwhile, the gradient was

prepared by mixing 4 ml 35% Na-tartrate solution with 5 ml 15% Na-tartrate/30% glycerine solution in 0.04M sodium phosphate buffer pH7.4, using a gradient mixer and Beckman Ultra-Clear™ centrifuge tubes (14×89 mm). Following centrifugation, the pellets were resuspended in 1 ml 1× PBS. The suspensions were applied to the tubes on top of the gradients. Centrifugation was performed at 91,000 ***g*** (60 min, 10 °C) in a SW41 rotor. After the centrifugation, the bands, corresponding to virions and Dense Bodies were visualized by light scattering and collected from the gradient, using a syringe and a 18G×1,5"-gauge needle. Each sample was supplemented with 1× PBS to give a total volume of 10 ml. The samples were again centrifuged at 100,000 ***g*** (90 min, 10 °C) in a SW41 rotor to pellet the material. Following that centrifugation step, the pellets were resuspended in 50 µl PBS and subsequently stored at −80 °C until further use.

Quantitative DNA-PCR analysis

Viral genome replication was performed as described before [21]. Extraction of viral DNA from infected cells was performed using the 'High Pure Viral Nucleic Acid' kit (Roche Life Science, Basel, Switzerland) according to the manufacturer's instructions. The DNA was finally eluted in 50 µl elution buffer and subjected to TaqMan analysis using an Applied Biosystems 7500 Real-Time PCR System (Life Technologies GmbH).

Statistical analyses

Statistical analyses were performed using two-tailed Welch's t-tests with Holm adjustment for multiple comparisons in R (version 4.1.2; R Foundation for Statistical Computing, Vienna, Austria).

RESULTS

Genome replication and cellular distribution of pp65 differs between HCMV strains RV-TB40$_{KL7}$ and HB5 (AD169)

Infection of HFF with low-passage HCMV strains like TB40/e is characterized by the release of subpopulations of viral progeny with different capacities to infect fibroblasts and endothelial cells. This may be related to the expression of the envelope protein complex, consisting of gH/gL/UL128-131 (pentamer) [31], which is absent in laboratory strains like HB5, an Ad169 derivative. It was, however, unclear if low-passage isolates and laboratory strains show differences in the kinetics of viral DNA replication. We addressed this by infecting HFF cells with HB5 [32] and RV-TB40$_{KL7}$ [26]. Infection was adjusted to comparable genome copy numbers in the cells at 6 h after infection. From this starting point on, cell samples were collected at different times and were subjected to quantitative polymerase chain reaction, using TaqMan protocols (Fig. 1a). The levels of viral replication were clearly lower in RV-TB40$_{KL7}$-infected cells at all time points tested, compared to HB5-infected cells. We also addressed the subcellular localization of pp65 in late-stage infected fibroblasts, using indirect immunofluorescence analysis (Fig. 1b). The tegument protein was predominantly located in the cytoplasm of cells infected with HB5 for 6 days. In RV-TB40$_{KL7}$-infected cells, however, the pp65-specific signal was mainly found in the nucleus. Taken together, these results showed that RV-TB40$_{KL7}$ and the laboratory strain HB5 differ in both DNA replication kinetics and subcellular pp65 localization at late stages of infection.

Generation of a viral mutant that expresses a cytoplasmic version of pp65

The RV-TB40$_{KL7}$ strain showed reduced replication kinetics in fibroblasts, compared to the laboratory strain HB5. The viruses differ in the subcellular localization of pp65 at late stages of infection of fibroblasts. We thus tested the hypothesis that the migration of pp65 in infected cells had an impact on viral productivity.

The pp65 shuttles between the cytoplasm and the cell nucleus [17, 18]. Its nuclear import is mediated by three independent nls [8, 9], and the nuclear export is mediated by a nuclear export signal via interaction with the nuclear exportin Crm1 [17, 18]. To address the question of whether the nuclear import of pp65 had an impact on HCMV infection, the nls were inactivated in the strain RV-TB40$_{KL7}$ genome by BAC mutagenesis. Based on BAC-TB40$_{KL7}$ [26], a mutant was generated in which the basic AA in the nls of pp65 (nls1, nls2 [8] and nls3 [9]) were replaced by alanine residues (Fig. 2a). The respective virus was termed TB40-pp65*nls*. To verify the phenotype of this novel strain, HFFs were infected and stained for pp65 expression at 3 d.p.i. and 6 d.p.i., using indirect immunofluorescence analysis. Complete cytoplasmic pp65 retention was found at both investigated time points (Fig. 2b, c). Infection with RV-TB40$_{KL7}$ resulted in nuclear accumulation of pp65 at both 3 d.p.i. and 6 d.p.i. The data showed that the new viral strain displayed the expected phenotype for pp65 with respect to its subcellular location.

Different cell types show a markedly enhanced progeny production following infection with TB40-pp65*nls*

To test the hypothesis that the subcellular migration of pp65 in the course of infection was important for its productivity, different cell types were infected with either wt RV-TB40$_{KL7}$ or with TB40-pp65*nls*. Surprisingly, there was a statistically highly significant increase in progeny production in HFF and ARPE19 epithelial cells and a subtle increase in endothelial cells over time (Fig. 3a–c). These results were surprising and raised the question about the reason why pp65 would have developed into a nucleo-cytoplasmic shuttle protein which was not of advantage for HCMV replication.

(a)

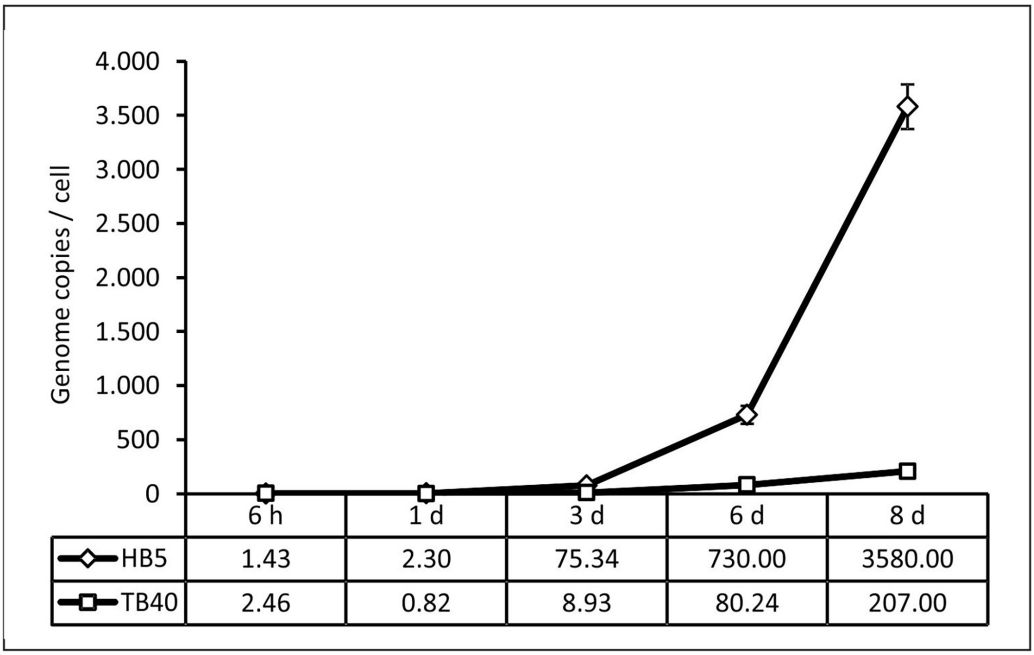

	6 h	1 d	3 d	6 d	8 d
HB5	1.43	2.30	75.34	730.00	3580.00
TB40	2.46	0.82	8.93	80.24	207.00

(b)

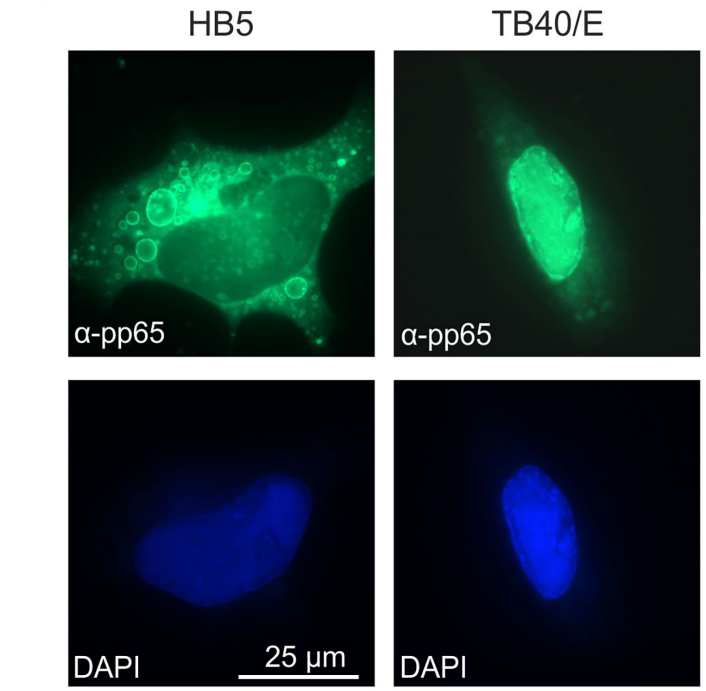

Fig. 1. Viral genome replication kinetics of laboratory strain HB5 (Ad169) and RV-TB40$_{KL7}$ (TB40) and subcellular localization of pp65 in infected HFF. (a) Cells were infected at a low m.o.i. of 0.05. Cell samples were collected at the indicated time points and analysed by quantitative DNA-PCR. The genome copies per cell are indicated both in the graph and in the table below. The experiment was performed once. (b) Cells were infected for 6 days. The localization of pp65 was analysed by indirect immunofluorescence analysis. Cell nuclei were stained with 4′,6-Diamidin-2-phenylindol

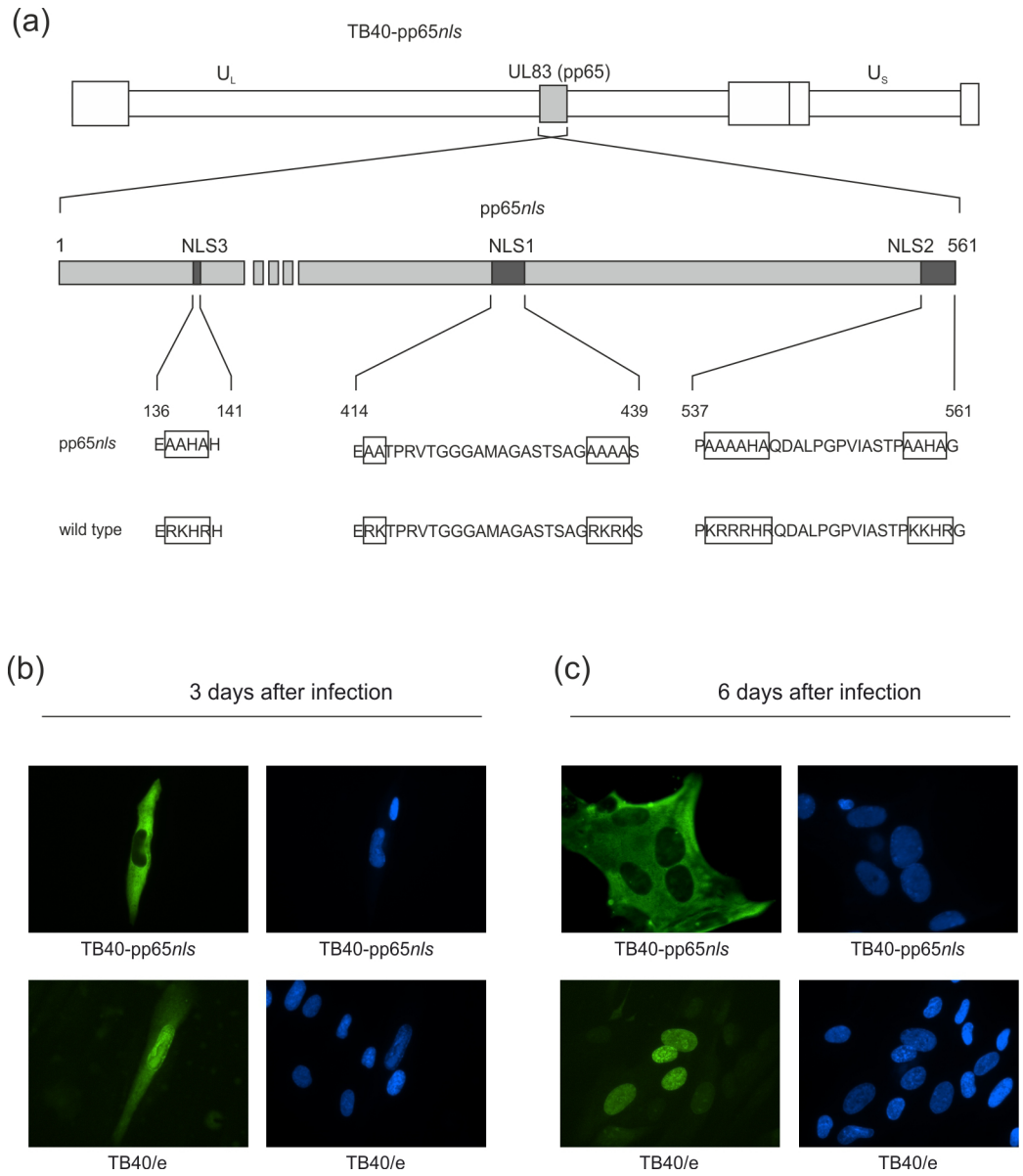

Fig. 2. Generation of an HCMV RV-TB40$_{KL7}$ strain variant with mutated nls. (a) Schematic illustration of the construction of TB40-pp65*nls*. The changes in the AA structure of pp65 are indicated by boxes. (b) Indirect immunofluorescence analysis of HFF, infected for 3 days with the indicated viruses. (c) Indirect immunofluorescence analysis of HFF, infected for 6 days with the indicated viruses. An antibody against pp65 was used for staining (green), and 4′,6-Diamidin-2-phenylindol was used to visualize cell nuclei. The experiment was performed once.

Previous studies had shown that the deletion of UL83 results in enhanced expression of the adjacent regulatory protein pp71, which in turn leads to increased viral genome replication [33]. The pp71 is known to be a multifunctional regulator of HCMV infection [34–40]. It stimulates the activity of the major immediate early gene IE1/IE2 but also affects early and late viral gene expression without affecting immediate early events, thereby markedly enhancing viral productivity [36, 41]. We thus addressed the question of whether the genetic manipulation that was required to replace the nls by alanine residues also resulted in deregulation of pp71 expression. HFFs were infected with RV-TB40$_{KL7}$ or TB40-pp65*nls*. Cell lysates were collected at different times after infection and subjected to Western blot analysis (Fig. 4a). Surprisingly, given the moderate alteration in UL83, TB40-pp65*nls*-infected cells expressed higher levels of pp71 compared to RV-TB40$_{KL7}$-infected cells (Fig. 4a). To see if that enhanced level of pp71 resulted in increased packaging of the tegument protein, virions were purified and tested by PAGE and silver staining (Fig. 4b). Both pp65 and pp71 were identified in the gel according to their known electrophoretic mobility in samples of purified virions [30, 42]. The results showed that pp71 levels were indeed enhanced in HCMV virion progeny of TB40-pp65*nls*. Surprisingly, very little pp65*nls* was found in these particles despite the fact that it was overexpressed in infected cells (Fig. 4a). Taken together,

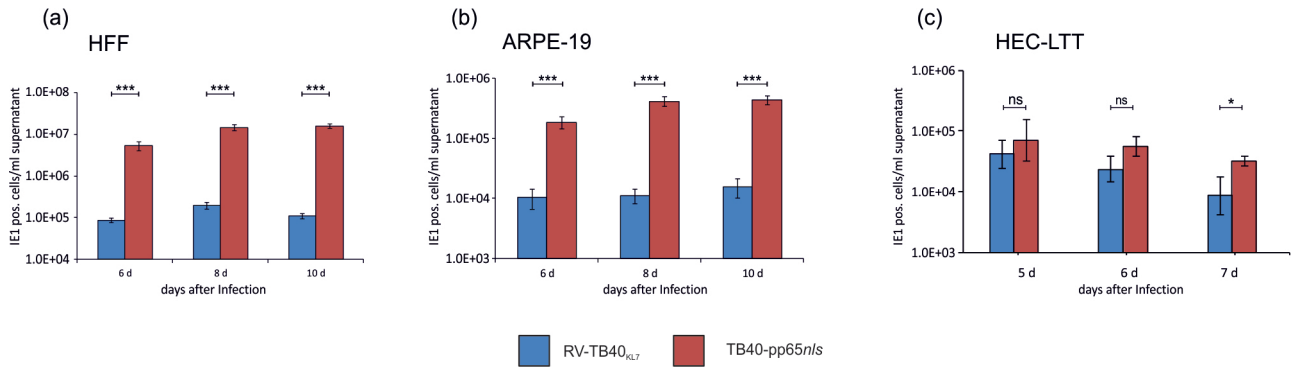

Fig. 3. Progeny production in HFF (a), ARPE-19 (b) and HEC-LTT (c) cells, following infection with RV-TB40$_{KL7}$ versus TB40-pp65*nls*. HFFs were infected with an m.o.i. of 4 genomes/cell, ARPE-19 were infected at 12.5 genomes/cell and HEC-LTT were infected with an m.o.i. of 3. Analyses were performed using the IE1 titration assay (a, b) or counting IE1-positive cells (c) on samples obtained at the indicated time points. Shown are means and deviations of eight independent technical replicates (a, b) or three independent biological replicates (c), respectively. RV-TB40$_{KL7}$ vs. TB40-pp65*nls* counts were compared at each time point using two-tailed Welch's t-tests. To account for multiple testing across three time points, *P*-values were adjusted using the Holm correction. NS, not significant; **P*<0.05, ***P*<0.01, ****P*<0.001.

the most likely explanation for the enhanced progeny production following TB40-pp65*nls* infection, compared to infection with RV-TB40$_{KL7}$ was an overexpression of pp71, but other effects, e.g. caused by unintended mutations in the BAC during genetic manipulation, cannot be excluded.

Expression of pp65*nls* from the UL1-UL6 gene locus of HCMV

The limited mutagenesis within the UL83 ORF of HCMV required to generate the TB40-pp65*nls* virus was, surprisingly, sufficient to deregulate the expression from the adjacent pp71-encoding UL82 reading frame. We thus were unable to discriminate possible

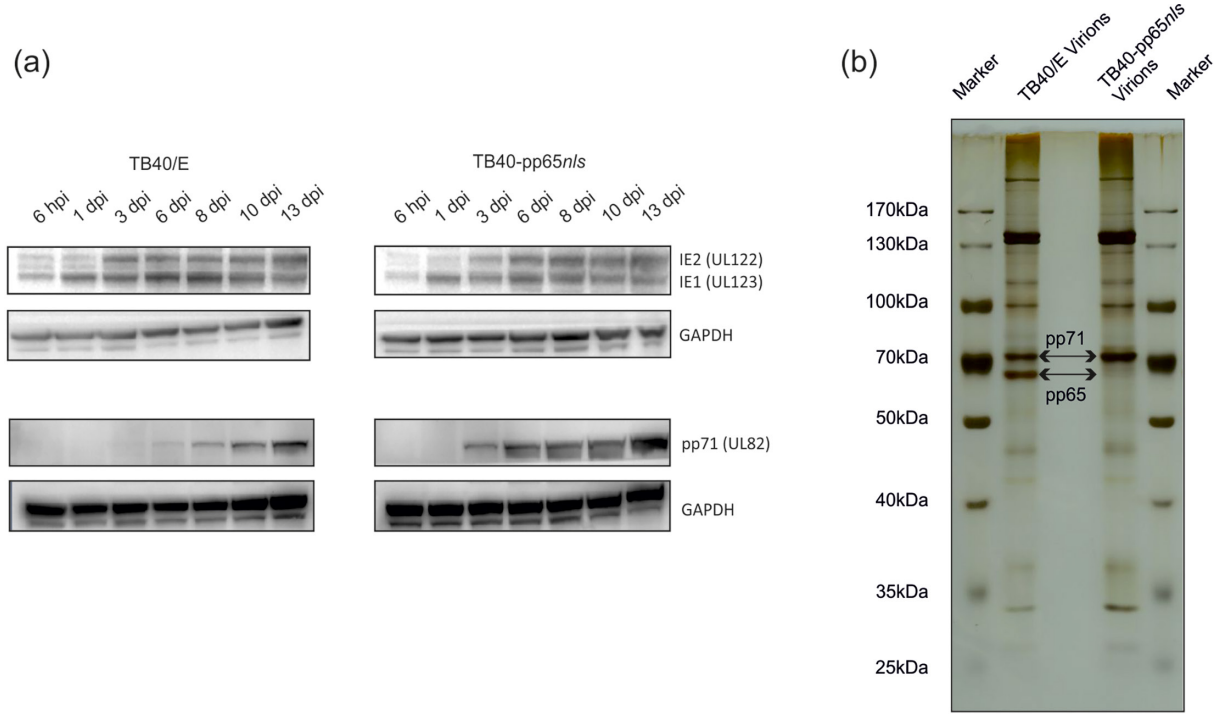

Fig. 4. Viral protein expression and packaging into virions, following infection with TB40-pp65*nls* or RV-TB40$_{KL7}$. (a) Immunoblot analysis of infected cell lysates, collected at the indicated times after infection. The filters were probed with antibodies against pp71 and against IE1 and IE2 of HCMV. GAPDH was carried along as a loading control. (b) Polyacrylamide gel analysis of purified virions from TB40-pp65*nls*-infected and RV-TB40$_{KL7}$-infected cells. The gel was silver stained. The putative locations of pp71 and pp65 in the gel are indicated by arrows. The experiments were performed once.

effects mediated by cytoplasmic pp65 retention from effects that might have been caused by the deregulation of pp71 expression or by other alterations caused by unintended mutations set somewhere else in the genome. To generate viruses with comparable levels of pp71 in an independent experiment, both the genes encoding either wt pp65 or pp65*nls* were inserted into the UL1-UL6 region of the viral mutant v65stop by BAC mutagenesis [25] (Fig. 5a). v65stop is a derivative of the TB40/E strain in which the expression of pp65 is abrogated by the insertion of two stop codons in the ORF of UL83, 30 bp downstream of the pp65 start codon [7]. The resulting recombinant viruses based on v65stop were reconstituted on HFF and tested by indirect immunofluorescence analysis for the expected location of pp65 (Fig. 5b). In addition, the intermediate BAC of v65stop containing the bacterial galK gene was also reconstituted. The respective virus v65stop-galK served as pp65-negative control.

Mutation of the nls of pp65 leads to a marked impairment of progeny release

To again test the impact of pp65 cytoplasmic retention on HCMV progeny production, HFFs were infected with v65stop-pp65*nls*. For control, cells were either infected with v65stop-pp65wt, expressing the wt pp65, or with v65stop-galk, lacking pp65 expression. Culture supernatants were collected at 5 d.p.i. and 7 d.p.i. and subjected to the IE1 titration assay to measure progeny release. v65stop-pp65*nls*-infected cells released significantly less progeny virus at 5 d.p.i. and 7 d.p.i., respectively, compared to v65stop-pp65wt-infected cells (Fig. 6). Cells infected with the pp65-null mutant also showed impairment in viral progeny production, yet, interestingly, to a lesser extent compared to v65stop-pp65*nls*. These data showed that both the abrogation of pp65 expression and the deletion of its nls lead to an impairment of progeny production.

Cytoplasmic retention of pp65 has little impact on pp71 packaging into virions

Initial experiments had shown that even subtle genetic alterations in the UL83 ORF of the HCMV genome may lead to over-expression of the adjacent pp71 gene UL82. This resulted in an increase in pp71 packaging into virions (Fig. 4b) and likely in increased viral progeny production (Fig. 3). To test if the expression of the pp65nls version of the tegument protein from a distant genomic location had a similar impact on virion composition, HFFs were infected with either v65stop-pp65*nls*, v65stop-pp65wt or v65stop-galk. Culture supernatants were collected at 7 d.p.i. Virions were purified by glycerol-gradient centrifugation. Samples of the three viruses showed similar banding patterns for virions and non-infectious enveloped particles (NIEPs) [3] in the gradient (Fig. 7a). Interestingly, no Dense Bodies were visible in the gradient of the particles from v65stop-pp65*nls*, similar to what was seen for the gradient for v65stop-galk. The latter was expected, as it is known that Dense Bodies are not formed in the absence of pp65. As Dense Body synthesis occurs in the cytoplasm, it remains unclear why no Dense Bodies were released from v65stop-pp65*nls*-infected cells despite the accumulation of pp65 in the cytoplasm. To test the protein composition of the particles, virions and Dense Bodies were subjected to SDS-PAGE. The resulting gel was stained by silver nitrate to visualize the protein bands (Fig. 7b). The pp71 band was identified according to its known electrophoretic mobility in samples of purified virions [30, 42]. Comparable amounts of pp71 were found in all three virion fractions, indicating that the genetic manipulations required to establish the mutant viruses had no impact on pp71 levels. A band corresponding to pp65 was only seen in v65stop-pp65wt virions. No pp65 was found in virions of the pp65-negative virus v65stop-galk. A pp65 band was also absent in the virion fraction of v65stop-pp65*nls*. This suggests that the nuclear location of pp65 during lytic infection, and likely also its nucleo-cytoplasmic shuttling function, was important for the uploading of the tegument protein into viral particles. Of note, one band at ~80 kDa was seen in the virions of v65stop-pp65wt, but not in the virions of the two other viruses. This band likely corresponds to pUL25. This protein interacts with pp65 and is dependent on the presence of pp65 for its packaging into virions [42]. The pattern of other viral proteins appeared to be comparable between the three viruses.

Mutation of the pp65 nls has little impact on the steady-state levels of DNA sensors IFI16 or cGAS or of ISG Mx1

pp65 interferes with the intrinsic defence response of the cell. It binds to the IFN-inducible protein IFI16 in the nucleus, thereby abrogating its DNA-sensing function and its downstream induction of antiviral cytokines [10]. IFI16 has thus been identified as an antiviral restriction factor that limits HCMV infection [43]. Furthermore, pp65 has also been found to interact with the cyclic GMP/AMP synthase (cGAS) to prevent its interaction with the stimulator of IFN genes (STING) and to inactivate the signalling pathway through cGAS/STING/IFN regulatory factor 3 (IRF3) [13]. The cGAS/STING/IRF3 pathway is important for the stimulation of IFN expression and the downstream activation of IFN-stimulated genes (ISGs). To address the issue, if the inability of pp65*nls* to enter the nucleus during HCMV infection had an impact on the antiviral function of the protein, we first addressed the steady-state levels of the DNA sensors IFI16 and cGAS and of the ISG Mx1. IFI16 levels were addressed since previous results had shown that pp65 transports IFI16 from the nucleus into the cytoplasm, thereby protecting it from degradation [12]. Thus, the inability of pp65 to enter the nucleus should abrogate this effect. cGAS levels were investigated since they are targeted and inhibited by pp65 at early times, but it was unclear if this interaction leads to destabilization of the sensor [13]. The Mx1 protein expression was investigated as this protein is a member of the virus-induced ISGs. The pp65 is known to reduce IFN-β induction early in infection [13]. HFFs were infected with the different viruses. Cell lysates of infected cells were collected at 1 d.p.i. and 3 d.p.i. and subjected to Western blot analysis (Fig. 8). Little differences were found in the levels of cGAS, IFI16 or Mx1 at 1 d.p.i. A slight difference was seen for IFI16 and cGAS, when their levels in v65stop-pp65wt-infected cells were compared to the levels in

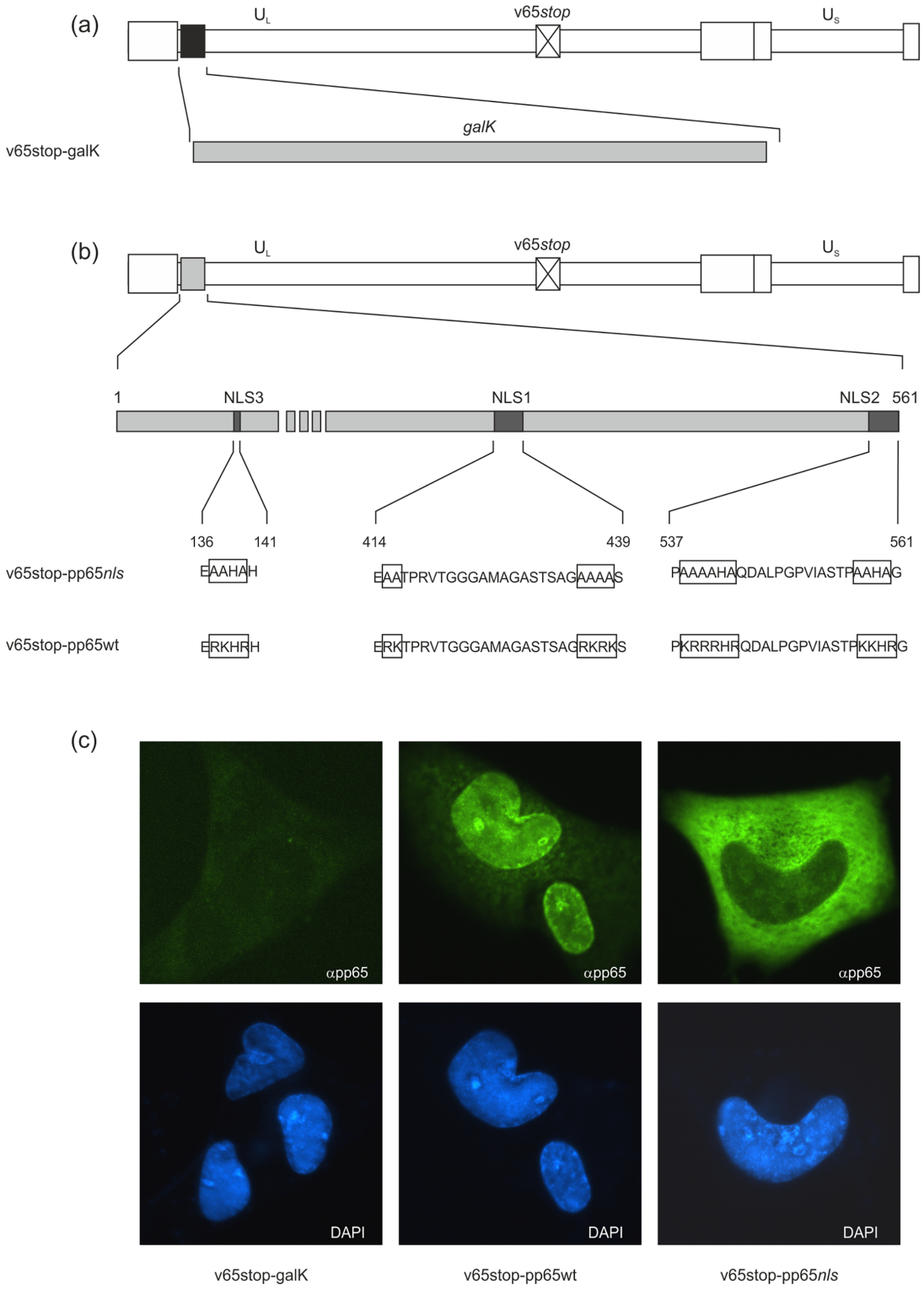

Fig. 5. Generation of HCMV mutants that express pp65 or pp65*nls* from the UL1-UL6 gene locus by BAC mutagenesis. (a) Schematic illustration of the insertion of the *galk* gene into the UL1-UL6 locus of v65stop, thereby replacing the latter genes. This virus is pp65-deficient. (b) Generation of v65stop mutants by replacing the *galk* gene with either the wt pp65 gene (v65stop-pp65wt) or pp65*nls* (v65stop-pp65*nls*). The changes in the AA structure of pp65 in dUL1-6-pp65*nls* are indicated by boxes. (c) Indirect immunofluorescence analysis of HFF, infected for 6 days with the indicated viruses. Staining was performed with a pp65-specific antibody (green) or with DAPI (4′,6-Diamidin-2-phenylindol). The experiment was performed once.

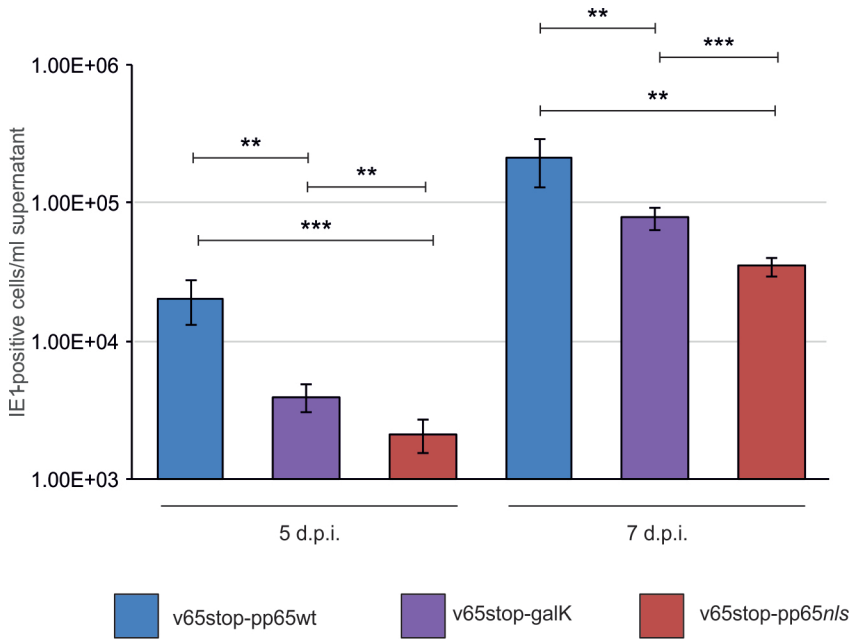

Fig. 6. Progeny production in HFF following infection with the three different viruses as indicated. Cells were infected with four genomes/cell. The cell culture supernatants were harvested at the indicated times and subjected to the IE1 titration assay. The number of IE1-positive cells correlates with the release of infectious progeny. v65stop-pp65wt, v65stop-galK and v65stop-pp65*nls* counts were compared at each time point using two-tailed Welch's t-tests for all pairwise contrasts. To account for multiple testing within each time point, *P*-values were adjusted using the Holm correction. $^{**}p<0.01$, $^{***}p < 0.001$. The results were confirmed in three independent experiments.

v65stop-pp65nls-infected cells or pp65-vstop-infected cells. The levels of both proteins appeared to be slightly decreased in cells infected with the latter two viruses. No differences were detectable in the levels of Mx1 when infected cell lysates of HFF were compared. Of note, there were clearly reduced steady-state levels of pp65 detectable in V65stop-pp65*nls*-infected cells, compared to the wt situation at 3 d.p.i. (Fig. 8), indicating enhanced degradation of the cytoplasmic pp65. In addition, there were reduced steady-state levels of IFI16 in 3 d.p.i. infected cells, irrespective of the strain used. Thus, although IFI16 may be stable at very early times [10, 44], it appears to be degraded at later times of HCMV infection independent of pp65 expression. Of note, IFI16 is also degraded in the course of herpes simplex virus infection [45].

HCMV progeny production is comparable between v65stop-pp65*nls* and v65stop-galK in cGAS and IFI16 knockout cells

The steady-state levels of pp65 differed markedly in cells infected with either v65stop-wt or v65stop-pp65*nls*. For that reason, it was impossible to exclude that the differences in pp65 levels had an impact on ISG levels seen in Fig. 8 unrelated to the location of the tegument protein. To address the question of whether the impaired progeny production following v65stop-pp65*nls* infection was related to a failure to interact with nuclear IFI16 or impaired interaction with cGAS, we thus infected HFF in which these genes were knocked out [46], using the same strain for each experiment. Cell culture supernatants from cells infected with v65stop-pp65*nls*, v65stop-pp65wt or v65stop-galk were collected at 7 d.p.i. The supernatants were subjected to the IE1 titration assay to measure progeny release.

No differences were found in progeny production when either HFF-ko IFI16 or HFF was infected with vpp65stop-*nls* (Fig. 9a). This indicated that IFI16 had no impact on the replication of this virus. There was also no difference seen when the same cells were infected with v65stop-galK (Fig. 9b), but enhanced progeny production from HFF-ko IFI16 following infection with v65stop-wt (Fig. 9c). These results showed that pp65 was required for the abrogation of nuclear IFI16 function and that the prevention of nuclear entry of pp65 prevented that inhibitory effect of pp65 on that protein. These results also showed that the reduced level of v65stop-pp65*nls* progeny production in HFF compared to v65stop-galK or v65stop-pp65wt (see Fig. 6) was independent of IFI16.

Infection of HFF-ko cGAS with v65stop-*nls*, in contrast, led to significantly higher levels of progeny production, compared to infection of HFF (Fig. 9a). The differences in progeny production, however, appeared to be in the same range as the differences seen after infection with the pp65-negative strain v65stop-galK (Fig. 9b). Thus, irrespective of whether pp65 was absent or expressed with the nls mutated, the same repression of progeny production was seen in HFF, compared to cGAS-deficient HFF. This indicated that, irrespective of whether pp65 was cytoplasmic or absent, there was the same level of interference of HCMV

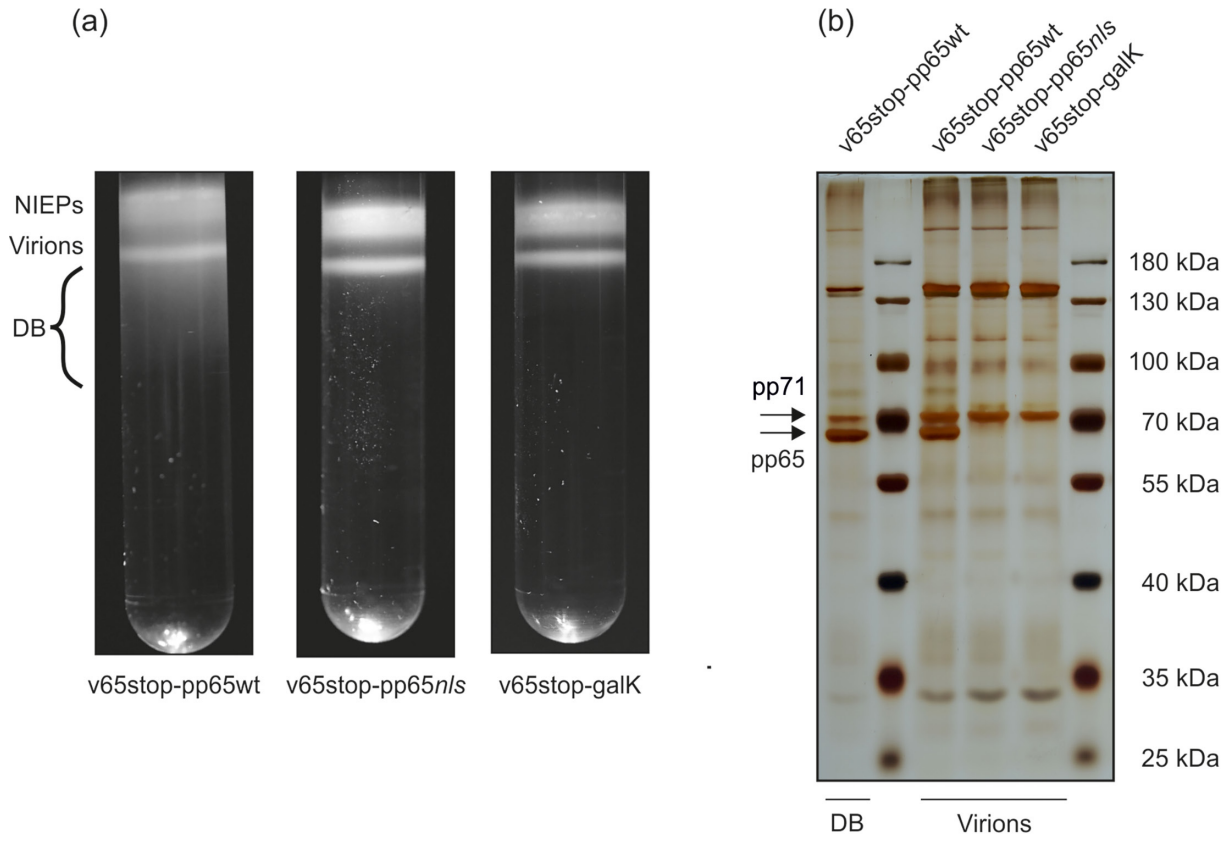

Fig. 7. Analysis of the protein content of virions of v65stop-pp65*nls*, v65stop-pp65wt, or v65stop-galk and of Dense Bodies (DB) from v65stop-pp65wt. (a) Gradients of viral particles, purified from infected HFF culture supernatants. The different fractions containing virions, NIEPs or Dense Bodies are visualized by light scattering. (b) Image of an SDS-polyacrylamide gel, used for the separation of the proteins of the virion and Dense Body fractions. The gel was stained with silver nitrate. No Dense Body fractions were seen in the gradients from v65stop-pp65*nls*- or v65stop-galk-infected cells; thus, only the Dense Body fraction from v65stop-pp65wt-infected cells is shown. Molecular mass markers were applied, the values of which are shown to the right. The locations of pp71 and pp65 in the gel are indicated by arrows. The experiment was performed once.

with cGAS and suggested that proteins other than pp65, such as pUL31, interfered with cGAS-mediated DNA sensing in this setting [47].

A viral strain that expressed the wt pp65 showed enhanced replication in HFF-ko cGAS and in HFF-ko IFI16, compared to its replication in wt HFF (Fig. 9c). The increase in progeny production was greater in HFF-ko cGAS compared to HFF-ko IFI16. Thus, concordant with the expectation, the deletion of either sensor allowed for an increase in viral productivity when wt pp65 was expressed.

Taken together, these experiments did not provide evidence that the reduction in progeny production in v65stop-pp65*nls*-infected cells was related to a defect of the mutated pp65 in its ability to interfere with cGAS- or IFI16-mediated DNA-sensing. The results also suggest that the interference of pp65 with the nuclear functions of IFI16 is dependent on its nuclear entry.

DISCUSSION

The pp65 is one of several HCMV tegument proteins that carry both structural and regulatory functions [3–5, 10, 12–16, 48–52]. One remarkable feature of the protein is its subcellular localization in the course of permissive HCMV infection. Driven by three nls, the pp65 accumulates in the nucleus immediately after infection. It subsequently shuttles between the nucleus and the cytoplasm [17, 18]. At early times of infection, it is preferentially detectable in the nucleus, indicating that the kinetics of nuclear import exceeds that of the export. As the infection progresses, pp65 accumulates in the cytoplasm of the cells. There are, however, HCMV strain-dependent differences in pp65 localization in the course of infection. Laboratory strains accumulate large pp65 amounts in the cytoplasm at late stages of infection, whereas cells infected with low-passage strains like TB40/E show a less pronounced cytoplasmic phenotype for pp65 at this time (see Fig. 1b). In previous work, we have created a virus expressing a mutant of pp65 with a primarily nuclear phenotype at all stages of infection [20]. This was accompanied by impairment of

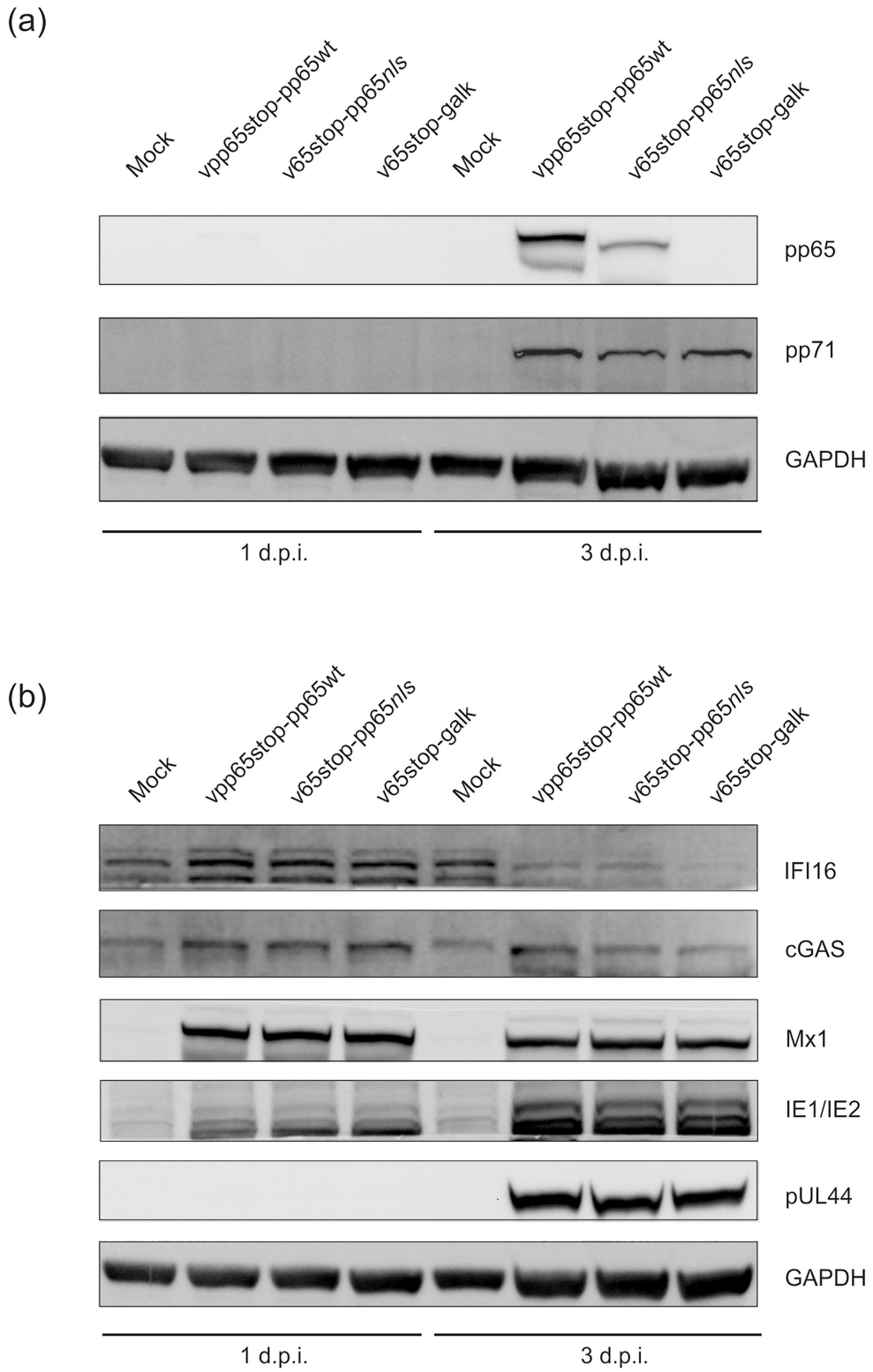

Fig. 8. Western blot analysis of the expression of selected viral proteins and of cGAS, IFI16 and Mx1 in HFF, infected for 1 day (1 d.p.i.) or 3 days (3 d.p.i.) with the different viruses. Mock, uninfected HFF. The proteins that were tested with specific antibodies are shown to the right. (a) Cell lysates were probed with antibodies against the viral proteins pp65 and pp71. GAPDH was stained as a loading control. (b) Cell lysates were probed with antibodies against the viral proteins IE1/IE2 and pUL44, as well as against IFI16, cGAS and Mx1. GAPDH was stained as a loading control.

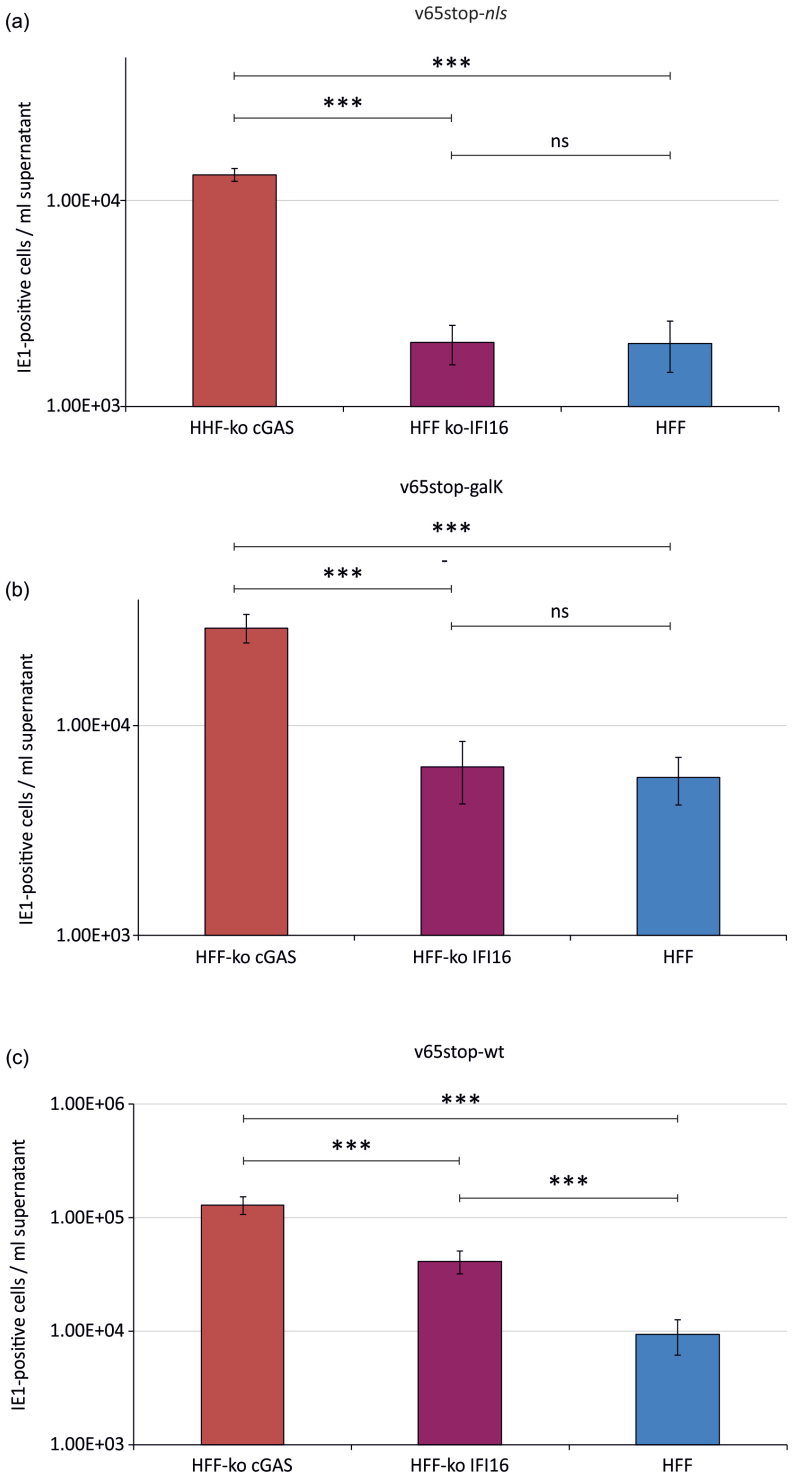

Fig. 9. Progeny production in HFF, HFF-ko IFI16 or HFF-ko cGAS, following infection with different viruses. Cells were infected at four genome copies/cell. The cell culture supernatants were harvested at 7 days after infection and subjected to the IE1 titration assay. The number of IE1-positive cells correlates with the release of infectious progeny. (a) Cells were infected with the v65stop-pp65*nls*, expressing the cytoplasmic version of pp65. (b) Cells were infected with the pp65-negative strain v65stop-galK. (c) Cells were infected with the pp65-expressing strain v65stop-wt. Counts in HHF, HFF-ko-IFI16 and HHF-ko-cGAS were compared for v65stop-nls, v65stop-galK and v65stop-wt, respectively, using two-tailed Welch's t-tests for all pairwise contrasts. To account for multiple testing across the three experiments per virus, *P*-values were adjusted using the Holm correction. NS, not significant; ***$P<0.001$. The experiment was performed independently twice with comparable results.

progeny production. It was expected that mutation of the pp65 nls would also impair viral productivity. In contrast, there was enhanced progeny production in HFF, epithelial cells and endothelial cells, when the nls of pp65 were mutated in UL83 upstream of the gene encoding the viral transactivator protein pp71. There were only subtle genetic modifications introduced in UL83, but still, this apparently led to an enhancement of the expression of the downstream pp71. The pp71 is a multifunctional protein that regulates HCMV infection on different levels [40]. By inserting a YFP-tagged version of pp71 into the HCMV backbone, Tavalai *et al*. showed that early and late protein expression was affected by the overexpression of that protein and the release of infectious virus was markedly increased [36]. In addition, Baldick *et al*. demonstrated that pp71 is capable of increasing the infectivity of transfected HCMV DNA through an effect that is separable from increased IE protein production [41]. Although it was not addressed here, it is likely that the unintended upregulation of pp71 was responsible for the enhancement of progeny production following TB40-pp65*nls* infection. Still, it cannot be excluded that unintended mutations in the HCMV genome during the genetic manipulation in bacteria were responsible for the effect.

Thus, the second set of HCMV mutants was generated to control for a possible impact of pp71 deregulation and for possible effects of inadvertent mutations in the BAC genomes. Using these viruses, progeny production by v65stop-pp65*nls*-infected cells was significantly lower, compared to v65stop-pp65wt-infected cells. This suggests that the nuclear localization and the shuttling function of pp65 were important for viral productivity. However, the changes in the primary structure of pp65 could as well have had an impact on protein–protein interaction. pp65 interacts with cytoplasmic cGAS and with nuclear IFI16, thereby compromising their function as DNA sensors [10, 13]. As pp65 interferes with these innate defence mechanisms of infected cells, the differences in progeny production between strains could have been related to different abilities to interact with innate responses. However, no differences were seen between the strains in the levels of ISG Mx1, suggesting that there were no differences in the IFN responses. Infection with v65stop-*nls* and the pp65-null mutant v65stop-galK in addition showed comparable impact on progeny production in HFF-cGAS ko and HFF-IFI16 ko cells. Although there was increased infectious progeny release from HFF-cGAS ko, the levels were comparable between the two viruses, indicating that the effect was unrelated to pp65. Other viral proteins like pUL31 have been described to interfere with cGAS sensing, thus likely explaining the effect [47]. And finally, no impact was observed on the levels of immediate-early or early viral proteins. Differences in the early cellular response to HCMV should have resulted in changes in viral replication and protein expression early on. This indicates that the viral replication progressed in a comparable way despite the cytoplasmic retention of pp65. Taken together, the experiments did not provide any evidence that the distinct reduction of infectious HCMV progeny released from v65stop-pp65*nls*-infected cells was related to an impairment of pp65 interference with innate defence mechanisms.

Besides its function as a regulatory protein that interferes with antiviral responses, pp65 is also an abundant structural component of infectious virions and of subviral Dense Bodies. It was originally considered to be an essential component during viral particle morphogenesis. Surprisingly, infectious virus is released from cells infected with pp65-null mutants [6]. However, the morphology of pp65-null virions appears to be altered, leading to enhanced detachment of the viral envelope from the tegument and likely an increase in altered, non-infectious virions [42]. This is in accordance with a reduced amount of functional, infectious v65stop-galK virions in the culture supernatant, compared to pp65-expressing strains (see Fig. 6). Similarly, reduced levels were seen following v65stop-pp65*nls* infection. This raises the question of whether the nucleo-cytoplasmic shuttling function of pp65 was important for virion morphogenesis and the quality of particles released from cells. pp65 is part of the outer tegument layer of mature HCMV virions. This layer is attached to the nascent virions in cytoplasmic viral assembly compartments (cVACs) [53]. The process appears to be impaired in v65stop-pp65*nls*-infected cells, as only limited amounts of the tegument protein are packaged into virions and no detectable amounts of Dense Bodies are released from the cells. It is unclear at this point why pp65*nls*, being already in the cytoplasm, was nevertheless inefficiently assembled into the tegument of nascent virions. However, the process of tegumentation is poorly defined for HCMV. Data from yeast and coimmunoprecipitation studies suggest that outer tegument assembly is mediated by a network of multiple protein interactions [54, 55]. Thus, the alteration in the pp65 structure in pp65*nls* could have led to an impairment of the ability of the protein to interact with other tegument proteins or with itself in the cytoplasm, thus leading to an impairment of morphogenesis in the cVACs. Remarkably, however, some of the most abundant tegument proteins, like pp65 (pUL83), pp71 (pUL82), pUL69 or pUL97, are mainly nuclear in the course of infection of human fibroblasts but may shift to the cytoplasm only at very late times of virion morphogenesis. We have recently shown that pp65 forms a nuclear complex with pUL69 and the viral kinase pUL97 [20]. pp65 is also known to locate to the nuclear egress complex likely by virtue of that interaction [56–58]. Thus, substructures of the viral tegument including pp65 may already be assembled in the nucleus. We could recently show that specific mutations in pp65 lead to the formation of aberrant pp65-pUL69-pUL97 containing nuclear complexes. This led to the accumulation of viral capsids in the nucleus, a failure of pp65 export and of Dense Body formation and a marked decrease of virus release [20]. It thus appears that the coordinated nuclear interaction of pp65 with other viral or cellular proteins is a prerequisite for proper virion morphogenesis. If such complexes are, however, exported from the nucleus, e.g. via their attachment to the surface of viral capsids formed in the nucleus, is unclear. Further experiments are required to test this.

Infection with v65stop-pp65*nls* led to reduced pp65 steady-state levels, compared to infection with v65stop-pp65wt. This could have been the reason for the reduction of v65stop-pp65*nls* progeny release from infected cells. However, progeny production was even lower than from cells infected with v65stop-galK, the pp65-negative control virus. Thus, a lack of pp65 function appears

to be unlikely. The limited packaging of pp65 into virions and the lack of Dense Bodies may rather be explained by the limited pp65 levels. However, pp65 was also below the level of detection in particles released from TB40-pp65*nls*-infected cells, although the levels of the protein were even higher in infected cells, compared to the control (see Fig. 4). In addition, significant amounts of pp65*nls* were detectable in the cytoplasm of v65stop-pp65*nls*-infected cells at late stages of infection (see Fig. 5). The levels of pp65*nls* are thus an unlikely explanation for the limited productivity of v65stop-pp65*nls* and the failure of upload of the tegument protein into viral particles.

There was a significantly reduced level of progeny production after infection with v65stop-galk compared to v65stop-pp65wt in repeated experiments. This is opposed to what Chevillotte *et al*. found [7]. An issue may be that pp65 was expressed here independent of the likely bicistronic UL83-UL82 gene. Alternatively, the insertion of UL83, driven by its own transcriptional regulatory elements, may have had some effect on neighbouring genes in the UL1-UL6 gene region used for insertion. The UL83 promoter is lacking in v65stop-galK. As, however, v65stop-pp65*nls*- and v65stop-pp65wt expression was driven by the same UL83 promotor, any putative influence on neighbouring genes should have been comparable.

Taken together, the nuclear localization of pp65 and its ability to shuttle between the nucleus and the cytoplasm and likely its ability to interact with viral and cellular proteins in the different compartments appear to be important for the levels of infectious progeny production. There is little evidence that this is related to its function in the impairment of antiviral defence functions. The intracellular trafficking of the tegument protein and its interaction with other viral proteins may be important for the complex orchestration of viral morphogenesis. Further studies will have to address the interaction of pp65 with viral structural components and the linkage of tegument protein interactions in the nucleus and the tegument assembly in the cVACs.

Funding information
The work was funded by grants from the Deutsche Forschungsgemeinschaft, individual project PL 236/7-1 (B.P.).

Acknowledgements
We are grateful to Christian Sinzger for providing TB40-BAC$_{KL7}$, to Jens von Einem for providing v65stop, to Dagmar Wirth for providing HEC-LTT and to William Britt for providing monoclonal antibodies.

Author contributions
Conceptualization: B.P. Funding acquisition: B.P. Investigation: N.B., C.S., C.Z. and C.L. Supervision: B.P. Validation: B.P. and H.S. Statistical analysis: H.S. Visualization: N.B., C.S. and B.P. Writing – original draft: B.P. and H.S. Writing – review and editing: B.P., N.B., C.S. and H.S.

Conflicts of interest
The authors declare that there are no conflicts of interest.

References

1. Boppana SB, Britt WJ. Synopsis of Clinical Aspects of Human Cytomegalovirus Disease. In: Reddehase MJ (eds). *Cytomegaloviruses From Molecular Pathogenesis to Intervention*, vol. 2. Norfolk, UK: Caister Academic Press; 2013. pp. 1–25.
2. Griffiths PD, Reeves M. Cytomegalovirus. In: Richman D, Whitley RJ and Hayden FG (eds). *Clinical Virology*, 4 ed. Washington, D.C: ASM Press; 2017. pp. 481–510.
3. Roby C, Gibson W. Characterization of phosphoproteins and protein kinase activity of virions, noninfectious enveloped particles, and dense bodies of human cytomegalovirus. *J Virol* 1986;59:714–727.
4. Varnum SM, Streblow DN, Monroe ME, Smith P, Auberry KJ, *et al*. Identification of proteins in human cytomegalovirus (HCMV) particles: the HCMV proteome. *J Virol* 2004;78:10960–10966.
5. Reyda S, Büscher N, Tenzer S, Plachter B. Proteomic analyses of human cytomegalovirus strain AD169 derivatives reveal highly conserved patterns of viral and cellular proteins in infected fibroblasts. *Viruses* 2014;6:172–188.
6. Schmolke S, Kern HF, Drescher P, Jahn G, Plachter B. The dominant phosphoprotein pp65 (UL83) of human cytomegalovirus is dispensable for growth in cell culture. *J Virol* 1995;69:5959–5968.
7. Chevillotte M, Landwehr S, Linta L, Frascaroli G, Lüske A, *et al*. Major tegument protein pp65 of human cytomegalovirus is required for the incorporation of pUL69 and pUL97 into the virus particle and for viral growth in macrophages. *J Virol* 2009;83:2480–2490.
8. Schmolke S, Drescher P, Jahn G, Plachter B. Nuclear targeting of the tegument protein pp65 (UL83) of human cytomegalovirus: an unusual bipartite nuclear localization signal functions with other portions of the protein to mediate its efficient nuclear transport. *J Virol* 1995;69:1071–1078.
9. Gallina A, Percivalle E, Simoncini L, Revello MG, Gerna G, *et al*. Human cytomegalovirus pp65 lower matrix phosphoprotein harbours two transplantable nuclear localization signals. *J Gen Virol* 1996;77 (Pt 6):1151–1157.
10. Li T, Chen J, Cristea IM. Human cytomegalovirus tegument protein pUL83 inhibits IFI16-mediated DNA sensing for immune evasion. *Cell Host Microbe* 2013;14:591–599.
11. Huang Y, Liu L, Ma D, Liao Y, Lu Y, *et al*. Human cytomegalovirus triggers the assembly of AIM2 inflammasome in THP-1-derived macrophages. *J Med Virol* 2017;89:2188–2195.
12. Biolatti M, Dell'Oste V, Pautasso S, von Einem J, Marschall M, *et al*. Regulatory interaction between the cellular restriction factor IFI16 and viral pp65 (pUL83) modulates viral gene expression and IFI16 protein stability. *J Virol* 2016;90:8238–8250.
13. Biolatti M, Dell'Oste V, Pautasso S, Gugliesi F, von Einem J, *et al*. Human cytomegalovirus tegument protein pp65 (pUL83) dampens type i interferon production by inactivating the DNA sensor cGAS without affecting STING. *J Virol* 2018;92:e01774-17.
14. Biolatti M, Dell'Oste V, Scutera S, Gugliesi F, Griffante G, *et al*. The viral tegument protein pp65 impairs transcriptional upregulation of IL-1β by human cytomegalovirus through inhibition of NF-kB activity. *Viruses* 2018;10:567.
15. Biolatti M, Dell'Oste V, De Andrea M, Landolfo S. The human cytomegalovirus tegument protein pp65 (pUL83): a key player in innate immune evasion. *New Microbiol* 2018;41:87–94.
16. Cristea IM, Moorman NJ, Terhune SS, Cuevas CD, O'Keefe ES, *et al*. Human cytomegalovirus pUL83 stimulates activity of the viral

immediate-early promoter through its interaction with the cellular IFI16 protein. *J Virol* 2010;84:7803–7814.

17. Frankenberg N, Lischka P, Pepperl-Klindworth S, Stamminger T, Plachter B. Nucleocytoplasmic shuttling and CRM1-dependent MHC class I peptide presentation of human cytomegalovirus pp65. *Med Microbiol Immunol* 2012;201:567–579.
18. Sanchez V, Mahr JA, Orazio NI, Spector DH. Nuclear export of the human cytomegalovirus tegument protein pp65 requires cyclin-dependent kinase activity and the Crm1 exporter. *J Virol* 2007;81:11730–11736.
19. Klages S, Rüger B, Jahn G. Multiplicity dependent expression of the predominant phosphoprotein pp65 of human cytomegalovirus. *Virus Res* 1989;12:159–168.
20. Becke S, Fabre-Mersseman V, Aue S, Auerochs S, Sedmak T, *et al*. Modification of the major tegument protein pp65 of human cytomegalovirus inhibits virus growth and leads to the enhancement of a protein complex with pUL69 and pUL97 in infected cells. *J Gen Virol* 2010;91:2531–2541.
21. Besold K, Wills M, Plachter B. Immune evasion proteins gpUS2 and gpUS11 of human cytomegalovirus incompletely protect infected cells from CD8 T cell recognition. *Virology* 2009;391:5–19.
22. Penner I, Büscher N, Krauter S, Plachter B. Subviral dense bodies of human cytomegalovirus enhance interferon-beta responses in infected cells and impair progeny production. *Viruses* 2023;15:1333.
23. Lieber D, Hochdorfer D, Stoehr D, Schubert A, Lotfi R, *et al*. A permanently growing human endothelial cell line supports productive infection with human cytomegalovirus under conditional cell growth arrest. *Biotechniques* 2015;59:127–136.
24. May T, Butueva M, Bantner S, Markusic D, Seppen J, *et al*. Synthetic gene regulation circuits for control of cell expansion. *Tissue Eng Part A* 2010;16:441–452.
25. Warming S, Costantino N, Court DL, Jenkins NA, Copeland NG. Simple and highly efficient BAC recombineering using galK selection. *Nucleic Acids Res* 2005;33:e36.
26. Sampaio KL, Weyell A, Subramanian N, Wu Z, Sinzger C. A TB40/E--derived human cytomegalovirus genome with an intact US-gene region and a self-excisable BAC cassette for immunological research. *Biotechniques* 2017;63:205–214.
27. Andreoni M, Faircloth M, Vugler L, Britt WJ. A rapid microneutralization assay for the measurement of neutralizing antibody reactive with human cytomegalovirus. *J Virol Methods* 1989;23:157–167.
28. Plachter B, Britt WJ, Vornhagen R, Stamminger T, Jahn G. Analysis of proteins encoded by IE regions 1 and 2 of human cytomegalovirus using monoclonal antibodies generated against recombinant antigens. *Virology* 1993;193:642–652.
29. Krömmelbein N, Wiebusch L, Schiedner G, Büscher N, Sauer C, *et al*. Adenovirus E1A/E1B transformed amniotic fluid cells support human cytomegalovirus replication. *Viruses* 2016;8:37.
30. Zimmermann C, Büscher N, Krauter S, Krämer N, Wolfrum U, *et al*. The abundant tegument protein pUL25 of human cytomegalovirus prevents proteasomal degradation of pUL26 and supports its suppression of ISGylation. *J Virol* 2018;92:e01180-18.
31. Scrivano L, Sinzger C, Nitschko H, Koszinowski UH, Adler B. HCMV spread and cell tropism are determined by distinct virus populations. *PLoS Pathog* 2011;7:e1001256.
32. Borst EM, Hahn G, Koszinowski UH, Messerle M. Cloning of the human cytomegalovirus (HCMV) genome as an infectious bacterial artificial chromosome in *Escherichia coli*: a new approach for construction of HCMV mutants. *J Virol* 1999;73:8320–8329.
33. Hesse J, Reyda S, Tenzer S, Besold K, Reuter N, *et al*. Human cytomegalovirus pp71 stimulates major histocompatibility complex class i presentation of IE1-derived peptides at immediate early times of infection. *J Virol* 2013;87:5229–5238.
34. Liu B, Stinski MF. Human cytomegalovirus contains a tegument protein that enhances transcription from promoters with upstream ATF and AP-1 cis-acting elements. *J Virol* 1992;66:4434–4444.
35. Schierling K, Stamminger T, Mertens T, Winkler M. Human cytomegalovirus tegument proteins ppUL82 (pp71) and ppUL35 interact and cooperatively activate the major immediate-early enhancer. *J Virol* 2004;78:9512–9523.
36. Tavalai N, Kraiger M, Kaiser N, Stamminger T. Insertion of an EYFP-pp71 (UL82) coding sequence into the human cytomegalovirus genome results in a recombinant virus with enhanced viral growth. *J Virol* 2008;82:10543–10555.
37. Kalejta RF, Shenk T. Proteasome-dependent, ubiquitin-independent degradation of the Rb family of tumor suppressors by the human cytomegalovirus pp71 protein. *Proc Natl Acad Sci USA* 2003;100:3263–3268.
38. Kalejta RF, Shenk T. The human cytomegalovirus UL82 gene product (pp71) accelerates progression through the G1 phase of the cell cycle. *J Virol* 2003;77:3451–3459.
39. Scherer M, Stamminger T. Emerging role of PML nuclear bodies in innate immune signaling. *J Virol* 2016;90:5850–5854.
40. Kalejta RF, Albright ER. Expanding the known functional repertoire of the human cytomegalovirus pp71 protein. *Front Cell Infect Microbiol* 2020;10:95.
41. Baldick CJ Jr, Marchini A, Patterson CE, Shenk T. Human cytomegalovirus tegument protein pp71 (ppUL82) enhances the infectivity of viral DNA and accelerates the infectious cycle. *J Virol* 1997;71:4400–4408.
42. Reyda S, Tenzer S, Navarro P, Gebauer W, Saur M, *et al*. The tegument protein pp65 of human cytomegalovirus acts as an optional scaffold protein that optimizes protein uploading into viral particles. *J Virol* 2014;88:9633–9646.
43. Gariano GR, Dell'Oste V, Bronzini M, Gatti D, Luganini A, *et al*. The intracellular DNA sensor IFI16 gene acts as restriction factor for human cytomegalovirus replication. *PLoS Pathog* 2012;8:e1002498.
44. Lin KM, Nightingale K, Soday L, Antrobus R, Weekes MP. Rapid degradation pathways of host proteins during HCMV infection revealed by quantitative proteomics. *Front Cell Infect Microbiol* 2020;10:578259.
45. Orzalli MH, DeLuca NA, Knipe DM. Nuclear IFI16 induction of IRF-3 signaling during herpesviral infection and degradation of IFI16 by the viral ICP0 protein. *Proc Natl Acad Sci USA* 2012;109:E3008–17.
46. Penner I, Büscher N, Dejung M, Freiwald A, Butter F, *et al*. Subviral dense bodies of human cytomegalovirus induce an antiviral type I interferon response. *Cells* 2022;11:4028.
47. Huang Z-F, Zou H-M, Liao B-W, Zhang H-Y, Yang Y, *et al*. Human cytomegalovirus protein UL31 inhibits DNA sensing of cGAS to mediate immune evasion. *Cell Host Microbe* 2018;24:69–80.
48. Kalejta RF. Functions of human cytomegalovirus tegument proteins prior to immediate early gene expression. *Curr Top Microbiol Immunol* 2008;325:101–115.
49. Smith RM, Kosuri S, Kerry JA. Role of human cytomegalovirus tegument proteins in virion assembly. *Viruses* 2014;6:582–605.
50. Stempel M, Chan B, Brinkmann MM. Coevolution pays off: Herpesviruses have the license to escape the DNA sensing pathway. *Med Microbiol Immunol* 2019;208:495–512.
51. Abate DA, Watanabe S, Mocarski ES. Major human cytomegalovirus structural protein pp65 (ppUL83) prevents interferon response factor 3 activation in the interferon response. *J Virol* 2004;78:10995–11006.
52. Browne EP, Shenk T. Human cytomegalovirus UL83-coded pp65 virion protein inhibits antiviral gene expression in infected cells. *Proc Natl Acad Sci U S A* 2003;100:11439–11444.
53. Sanchez V, Greis KD, Sztul E, Britt WJ. Accumulation of virion tegument and envelope proteins in a stable cytoplasmic compartment during human cytomegalovirus replication: characterization of a potential site of virus assembly. *J Virol* 2000;74:975–986.

54. To A, Bai Y, Shen A, Gong H, Umamoto S, *et al*. Yeast two hybrid analyses reveal novel binary interactions between human cytomegalovirus-encoded virion proteins. *PLoS One* 2011;6:e17796.
55. Phillips SL, Bresnahan WA. Identification of binary interactions between human cytomegalovirus virion proteins. *J Virol* 2011;85:440–447.
56. Kamil JP, Coen DM. Human cytomegalovirus protein kinase UL97 forms a complex with the tegument phosphoprotein pp65. *J Virol* 2007;81:10659–10668.
57. Milbradt J, Kraut A, Hutterer C, Sonntag E, Schmeiser C, *et al*. Proteomic analysis of the multimeric nuclear egress complex of human cytomegalovirus. *Mol Cell Proteomics* 2014;13:2132–2146.
58. König P, Büscher N, Steingruber M, Socher E, Sticht H, *et al*. Dynamic regulatory interaction between cytomegalovirus major tegument protein pp65 and protein kinase pUL97 in intracellular compartments, dense bodies and virions. *J Gen Virol* 2017;98:2850–2863.